Low effect of phenanthrene bioaccessibility on its biodegradation in diffusely contaminated soil

M. Crampon, A. Cébron, F. Portet-Koltalo, S. Uroz, F. Le Derf, J. Bodilis

▶ **To cite this version:**

M. Crampon, A. Cébron, F. Portet-Koltalo, S. Uroz, F. Le Derf, et al.. Low effect of phenanthrene bioaccessibility on its biodegradation in diffusely contaminated soil. Environmental Pollution, 2017, 225, pp.663-673. 10.1016/j.envpol.2017.03.053 . hal-01597866

HAL Id: hal-01597866
https://hal.science/hal-01597866

Submitted on 21 Jan 2022

HAL is a multi-disciplinary open access archive for the deposit and dissemination of scientific research documents, whether they are published or not. The documents may come from teaching and research institutions in France or abroad, or from public or private research centers.

L'archive ouverte pluridisciplinaire **HAL**, est destinée au dépôt et à la diffusion de documents scientifiques de niveau recherche, publiés ou non, émanant des établissements d'enseignement et de recherche français ou étrangers, des laboratoires publics ou privés.

Distributed under a Creative Commons Attribution - NonCommercial - NoDerivatives 4.0 International License

Low effect of phenanthrene bioaccessibility on its biodegradation in diffusely contaminated soil

M. Crampon[a,b], A. Cébron[c,d], F. Portet-Koltalo[a], S. Uroz[e], F. Le Derf[a], J. Bodilis[b,f#]

[a] COBRA UMR CNRS 6014, Université de Rouen-Normandie, 55 rue saint Germain, 27000 Evreux, France

[b] Laboratoire de Microbiologie Signaux et Microenvironnement, EA 4312, Université de Rouen, 76821 Mont Saint Aignan, France

[c] CNRS, LIEC UMR 7360, Faculté des Sciences et Technologies, BP70239, 54506 Vandoeuvre-lès-Nancy Cedex, France

[d] Université de Lorraine, LIEC UMR 7360, Faculté des Sciences et Technologies, BP70239, 54506 Vandoeuvre-lès-Nancy Cedex, France

[e] UMR 1138 INRA, centre de Nancy, Biogéochimie des Ecosystèmes forestiers, Route d'Amance, 54280 Champenoux, France

[f] Université de Lyon, France; CNRS, INRA, Ecole Nationale Vétérinaire de Lyon, and Université Lyon 1, UMR 5557 Ecologie Microbienne, 43 boulevard du 11 novembre 1918, 69622 Villeurbanne cedex, France

Short title: Low effect of bioaccessibility on phenanthrene biodegradation in soil

Corresponding author: J. Bodilis, josselin.bodilis@univ-rouen.fr

Keywords: phenanthrene biodegradation; soil; bioaccessibility; DNA-SIP; rhamnolipids; *Rhodocyclaceae*

Graphical Abstract

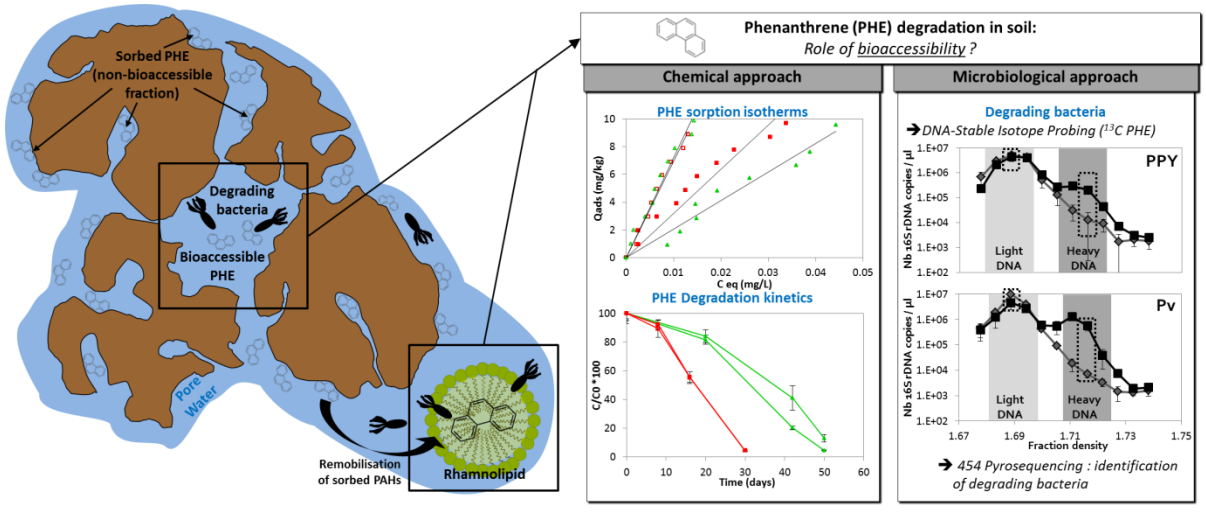

Abstract

This study focused on the role of bioaccessibility in the phenanthrene (PHE) biodegradation in diffusely contaminated soil, by combining chemical and microbiological approaches. First, we determined PHE dissipation rates and PHE sorption/desorption kinetics for two soils (PPY and Pv) presenting similar chronic PAH contamination, but different physico-chemical properties. Our results revealed that the PHE dissipation rate was significantly higher in the Pv soil compared to the PPY soil, while PHE sorption/desorption kinetics were similar. Interestingly, increases of PHE desorption and potentially of PHE bioaccessibility were observed for both soils when adding rhamnolipids. Second, using ^{13}C-PHE incubated in the same soils, we analysed the PHE degrading bacterial communities. The combination of stable isotope probing (DNA-SIP) and 16S rRNA gene pyrosequencing revealed that *Betaproteobacteria* were the main PHE degraders in the Pv soil, while a higher bacterial diversity (*Alpha-*, *Beta-*, *Gammaproteobacteria* and *Actinobacteria*) was involved in PHE degradation in the PPY soil. The amendment of biosurfactants commonly used in biostimulation methods (*i.e.* rhamnolipids) to the two soils clearly modified the PHE sorption/desorption kinetics, but had no significant impact on PHE degradation rates and PHE-degraders identity. These results demonstrated that

increasing the bioaccessibility of PHE has a low impact on its degradation and on the functional populations involved in this degradation.

Capsule

The increase of the bioaccessibility level of phenanthrene has a low impact on its degradation in diffusely contaminated soil.

Introduction

Polycyclic aromatic hydrocarbons (PAHs) are ubiquitous carcinogenic organic contaminants, originating from multiple sources (*i.e.* biogenic, petrogenic and pyrogenic). Among them, human activities are responsible for the major releases into the environment, particularly through atmospheric deposition (Tobiszewski and Namieśnik, 2012). PAHs physico-chemical properties (high chemical stability, low vapor pressure, low aqueous solubility, high water-organic carbon K_{oc} partition coefficient) make them persistent in soils. However, this persistence is also strongly dependent on soil physico-chemical properties and soil microbial activities (Doyle et al., 2008).

In the case of diffuse contamination, soils are continuously exposed to low and repeated deposits of PAHs. In these soils, PAHs can be found in different soil compartments, depending on the age and history of the contamination. A small fraction of these PAHs is usually present in the soil aqueous phase, and is considered as directly accessible to microorganisms for degradation. The bioaccessible fraction is available to cross cellular membranes if the organism is present and has access to it, even after a period of time or through spatial rearrangements, whereas the bioavailable fraction is that is freely available to cross the organism's cellular membrane at a given time (Riding et al., 2013). The PAHs recently adsorbed on soil constituents are also generally directly accessible to microorganisms, while PAHs in contact with soil constituents for a longer time become poorly bioaccessible. A last fraction of PAHs can be strongly bound to soils, by slow diffusion into soil micropores. The strong sorption/sequestration mechanisms of PAHs to organo-mineral complexes eventually creates non-extractable bound-residues (Ahangar, 2010), considered as not bioaccessible (Semple et al., 2004).

After adaptation and selection processes, the soil bacterial communities acquire the potential to biodegrade the bioaccessible PAH fraction (Haritash and Kaushik, 2009). Indeed, different bacterial strains isolated from various contaminated soils have been described as capable of degrading PAHs and of growing with PAHs as sole carbon source. These bacteria belong to different phyla or classes such as *α*-, *β*- and *γ*-*Proteobacteria* (Haritash and Kaushik, 2009; Jeon et al., 2006; Kim and Jeon, 2009; Niepceron et al., 2013), *Bacteroidetes*, *Actinobacteria* (Timmis et al., 2010) or *Firmicutes* (Wu et al., 2008).

The bioaccessibility factor depends on the physico-chemical properties of PAH compounds and on the soil properties (clays and organic matter contents and nature) (Brandli et al., 2008; Jonker et al., 2005; Mechlińska et al., 2009; Xia et al., 2010). Besides that, the bioavailability factor depends on the physiological and catabolic potential of soil microorganisms (Crampon et al., 2014). The combination of these complex processes determines the fate of PAHs in soils (Semple et al., 2004; Semple et al., 2003). Enhancement of PAH bioaccessibility in contaminated soils through addition of surfactants has already been reported (Ahn et al., 2008; Paria, 2008; Zhou et al., 2007; Zhou and Zhu, 2008). Biosurfactants (*e.g.* surfactants naturally produced by (micro)organisms) are more environmental friendly and interesting due to their low critical micellar concentration (CMC) and their lower toxicity for soil microorganisms than synthetic ones (Bustamante et al., 2012). Rhamnolipids, produced by *Pseudomonas aeruginosa* (Bordas et al., 2005), have been described for their ability to remobilize sorbed PAHs and to potentially enhance their biodegradation in slurry batches or column experiments (Bordas et al., 2005; Congiu and Ortega-Calvo, 2014). However, the real impact of these rhamnolipids on PAHs accessibility after direct treatment of contaminated soils remains to be determined.

In this context, the aim of this study was to determine the parameters mostly governing phenanthrene (PHE) degradation rates in diffusely contaminated soils. PHE was chosen as a

model PAH representative of low molecular weight PAHs (2-3 fused aromatic rings). To address such an objective, two soil types (PPY and Pv) characterized by similar chronic PAH contamination, but different physico-chemical characteristics, were analyzed and compared. In each soil type, chemical and molecular biological methods were combined to investigate the fate of phenanthrene (PHE) by focusing on: (i) PHE accessibility, (ii) PHE degradation kinetics, and (iii) PHE-degrading bacterial diversity in relation to the amendment or not of rhamnolipids. PHE degradation was monitored using a microcosm approach during two months. In microcosm, PHE sorption isotherms with or without rhamnolipids were determined to estimate PHE accessibility. PHE degradation kinetics were determined using ^{13}C-PHE and PHE-degrading bacterial populations were identified through DNA-Stable Isotope Probing (DNA-SIP) and 16S rRNA gene amplicon pyrosequencing.

Materials and Methods

Soil sampling and soil analyses

Soil samples were collected in the Seine river basin (France), which is a highly urbanized and industrialized location accounting for 40% of the French economic activity and including 33% of oil refining and 50% of river traffic. In spring 2014, approximately 15 kg of soil (0–15 cm depth) of two diffusely contaminated soil types (PPY and Pv) were sampled. PPY soil is an agricultural soil characterized by a permanent grassland and located near Yvetot (Seine-Maritime department, 49°36'40.6"N 0°44'10.7"E), at about 15 km from the Seine River. The PPY soil is classified as Luvisol according to the World Reference Base for soil resources (IUSS Working Group WRB 2006). The second soil type sampled (Pv) is located near Petiville (Seine Maritime department, 49°25'54.0"N 0°36'25.4"E) in the Seine river estuary, and is

partially covered by young willow. This soil, periodically flooded, is classified as fluvic Gleysol according to the World Reference Base for soil resources.

After sampling, field-moist soils were sieved through a 5 mm mesh and stored at room temperature for 8 days for acclimation. Aliquots were stored at -20°C for molecular characterization of the initial microbial communities in the two soil types before PAH spiking. The natural background concentrations of PAHs in both soils were lower than 1 $mg.kg^{-1}$ for the sum of the 16 PAHs classified as priority by the US-Environmental Protection Agency (US-EPA) (Table 1).

Pv and PPY soil organic matter (OM) was analyzed on dried crushed soils by RockEval 6 pyrolysis (Vinci Technologies, France) and S2 peak deconvolution (Sebag et al., 2006) was obtained using peakfit software (SigmaPlot, Systat) and the "Bulk Rock" method, as described previously (Crampon et al., 2014) (Table 1). Nature of clays in soils was analyzed by X-Ray diffraction (XRD) (Philips PW3040 diffractometer, France), as described previously (Crampon et al., 2014).

Soil pH was determined according to the French NF ISO 10-390 standard. Granulometry was analyzed according to the NF X31-107 standard. CEC (Cationic Exchange Capacity) was obtained following the French NF ISO 31-130 standard by the cobaltihexamine method. The analyses of pH, texture and CEC were carried out at the LAS-INRA laboratory (Arras, France).

Phenanthrene sorption isotherm determination

Sorption isotherm experiments were performed for both soils as previously described (Groboillot et al., 2011), in the presence or not of rhamnolipids. Briefly, sorption reactors consisted in 4 g of soil sieved at 355 µm and mixed with 40 mL deionized water in glass tubes under magnetic agitation. Reactors were incubated at 25°C along the experiment and $HgCl_2$ ($500mg.L^{-1}$) was added as a biocide at the beginning of the experiment to avoid bacterial

degradation, which could decrease PHE concentration in water after many hours. PHE was then introduced in the reactors with a known volume of PHE stock solution (100 $mg.L^{-1}$ in acetonitrile), to obtain a range of concentrations (from 0.1 to 1 $mg.L^{-1}$), below its limit of solubility in water (*i.e.* 1.6 $mg.L^{-1}$). The volume of acetonitrile injected (<1% of the total volume) was low enough to have no impact on PHE sorption, as previously studied (Groboillot et al., 2011). To evaluate the remobilization capacity of rhamnolipids, the biosurfactant (AGAE Technologies (USA), 90% purity) was added as a powder in the reactors 5 h after the introduction of PHE, to a final concentration of 0.55 $g.L^{-1}$ (concentration ten times higher than its CMC of 0.05 $g.L^{-1}$) to ensure the formation of micelles in the aqueous phase. Five hours was chosen as the time to add the biosurfactant after PHE spiking because it was observed that a "quasi" plateau was reached for PHE sorption after this time (data not shown). Mixtures treated or not with rhamnolipids were stirred during 24 h at 25°C to be sure to reach thermodynamic equilibrium (time evaluated during preliminary tests) (Barnier et al., 2014). Thereafter, reactors were centrifuged at 7000 rpm during 20 min to recover the aqueous phase. The concentration of PHE at equilibrium in the aqueous phase after 24 h (C_{eq}) was then measured after solid-phase extraction (SPE) and analysis using high-performance liquid chromatography coupled with fluorescence detector (HPLC-FLD) as developed, in the section below. As our systems were closed, PHE spiked at t_0 was fully distributed between the water and the soil phases after 24h. So, the sorbed concentration (C_{ads}) was deduced knowing the initial PHE concentration C_o, following the equation $C_{ads} = C_0 - C_{eq}$. The K_d partition coefficients were then obtained from the slope of the isotherms.

Phenanthrene dissipation kinetics

Microcosms consisted of 4.5 g of dry equivalent fresh soil (90%) and 0.5 g of dry sterilized (autoclaved at 120°C for 20 min) soil (10%) spiked with ^{12}C-PHE (purity > 98%) or ^{13}C-PHE

(uniformly labeled $^{13}C_{14}$, 99 atom %; Sigma-Aldrich), mixed in a hermetically-closed 100 mL sterile glass flask. A PHE solution was prepared in acetone and spiked to the dry sterilized soils in order to obtain a final PHE concentration of 3,000 mg.kg^{-1} of soil. The dry sterilized soil was mixed under an extractor hood for 24 h to homogenize the PHE distribution and to evaporate the remaining acetone. After one week of stabilization at ambient temperature, the dry PHE contaminated and sterilized soil was mixed with the wet native soil (humidity of 24.1 and 31.7% wt of fresh soil for PPY and Pv soils, respectively) and gently homogenized to obtain final soil microcosms contaminated with PHE (300 mg.kg^{-1} dw soil). This spiked PHE final concentration was 337-940 times higher than the sum of the 16 USEPA background PAHs (Table 1) and 2000-2857 times higher than the concentration of the native 2-3 aromatic ring PAHs. So we could reasonably consider that the main effects of PAHs on our studied systems were mainly due to the addition of PHE at 300 mg.kg^{-1}, and so the impact of co-metabolism was negligible in our study. It was decided to add the initial spiked dried sterilized soil (10%) to the native wet soil (90%) after contact time of only 7 days, in order to avoid PHE dissipation in the initial spiked soil. Soil water content of each microcosm was adjusted with distilled water to 70% of its water holding capacity. It corresponded to a total of 43.5 g and 49.1 g of water per 100 g soil for PPY and Pv soils, respectively. Rhamnolipids were added to distilled water to a final concentration of 300 mg.kg^{-1} dw soil into half of the microcosms. Rhamnolipids correspond to a mixture of mono and di-rhamnolipids (R90 product). So the concentration of the added biosurfactant was around 0.61-0.69 g.L^{-1} in the water fraction, which was near the concentration tested in sorption studies. The flasks were opened once a week in sterile conditions for 15 min to renew the atmosphere, and were incubated at 20°C in static mode in a dark room. Analyses of microcosms were carried out after 0, 8, 16 and 30 days of incubation for Pv soil and after 0, 20, 42 and 50 days for PPY soil, based on the different PHE degradation rates evaluated through a preliminary experiment (data not shown). These different sampling

times between the two soils were chosen in order to be able to compare the labeled DNA between the two soils (in terms of percentage of dissipated PHE), to potentially have the same quantity of ^{13}C possibly incorporated into the degrading bacteria DNA. All the microcosms were performed in triplicates giving a total of 96 microcosms (2 soils, with and without rhamnolipids, 4 incubation times, 3 replicates and with ^{12}C and ^{13}C PHE). The experimental protocol is available in supplementary materials (Fig. S1).

Phenanthrene extraction and measurements

All organic solvents were purchased from Fisher Scientific (Illkirch, France) and were of HPLC grade. PHE extractions from soils were performed using the microwave accelerated extraction (MAE; Mars X, CEM Corporation, USA) as described previously (Portet-Koltalo et al., 2008). For PHE degradation kinetics, two aliquots of 1.5–2 g of wet soil were taken from each of the three microcosms (in triplicates) at each time point. Then at each studied time, 6 sub-samples of a soil without biosurfactant and 6 sub-samples of the same soil amended with biosurfactant were dried 24 h at 35°C (to avoid the semi volatile PAH loss) and crushed separately. One g of each of the 6 sub-samples was extracted simultaneously using MAE technique in 20 mL of an acetone/toluene 50/50 (v/v) mixture at 130°C for 30 min, at 1,200 W. So for each studied time, extraction yields were obtained from a mean of 6 values. To determine the PAHs concentration in native soils, 10 g of crushed dried soil were processed using MAE technique, with 40 mL of the acetone/toluene 50/50 mixture, in the same conditions as described above. After filtration (0.45 µm Teflon filters; Fisher Scientific, France), extracts were evaporated to reach a volume of 1.5 mL. An internal standard (10 µL of perdeuterated PHE at 100 $mg.L^{-1}$) was added to 990 µL of each extract before GC-MS analyses. Quantification analyses were performed using a 6850 gas chromatograph from Agilent (USA) fitted with a mass spectrometer (MS) detector (5975C, Agilent) and using a DB5-MS capillary column (60 m×0.25 mm inner diameter, film

thickness 0.25 µm; J&W Scientific, USA) according to Crampon *et al*. (Crampon et al., 2014). The mass detector (electron impact ionization 70 eV) operated in the selected ion monitoring (SIM) mode for better sensitivity. The detection and quantification thresholds, calculated respectively as 3 and 10 times the standard deviation of the blank sample noise, were 1.5 and 5 $\mu g.L^{-1}$, respectively. The mean recovery of PHE after MAE-GC-MS extraction and analysis was 90.0±7.0% (n=5).

PHE extractions from aqueous media were done by SPE using Strata-X cartridges (Phenomenex, Le Pecq, France). After cartridge conditioning and sample percolation (Portet-Koltalo et al., 2013), PHE was eluted with 5 mL methylene chloride, and was evaporated under nitrogen flow and recovered in 1 mL acetonitrile before HPLC analysis. PHE quantification was performed using a HPLC (Beckman Coulter, USA) coupled to a FLD (Prostar 363, Varian, USA) and using a C_{18} Envirosep PP column (150×4.6 mm, dp = 5 µm) (Phenomenex, Le Pecq, France) according to Portet-Koltalo *et al*. (Portet-Koltalo et al., 2013). Detection and quantification limits, calculated respectively as 3 and 10 times the standard deviation of the sample noise, were evaluated as 0.4 and 1.3 $\mu g.L^{-1}$, respectively. The mean recovery of PHE after SPE-HPLC-FLD extraction and analysis was 94.2±1.2% (n=5). Taking into account the concentration factor using SPE, the limit of quantification of PHE in the aqueous medium was 33 $ng.L^{-1}$. So PHE was preferentially measured in the aqueous medium after sorption experiments because SPE-HPLC-FLD allowed us to reach lowest concentrations than using GC-MS and because of the highest accuracy of the method.

^{13}C labeled DNA isolation

For DNA-based diversity analyses, samples were selected for further analysis according to the level of ^{13}C PHE degradation. Initial soils collected before spiking (triplicates) and soil samples collected during the experiment at 20% (DT20) and 90% of PHE degradation (DT90) were used

for soil genomic DNA extractions using the PowerSoil DNA isolation kit (Mo-Bio Laboratories) according to the manufacturer recommendations. Extracted DNA was quantified using NanoDrop 2000 (Thermo Scientific) and samples were stored at -20°C until analysis.

Heavy (^{13}C labeled) and light DNA (^{12}C) were separated according to the protocol described by Neufeld et al. (Neufeld et al., 2007). Gradients were prepared using a CsCl solution (purity ≥ 99%; Sigma-Aldrich) with an initial density of ca 1.85. Gradient buffer and DNA sample were then added (for a final DNA quantity in the centrifuge tube of 5 to 10 µg) to obtain a final density of 1.725. Ultracentrifugations were carried out on a Beckman centrifuge (Optima L-80 XP) with a vertical rotor Vti 65.2 (Beckman), at 42,400 rpm for 40 h at 20°C, with maximal acceleration and no deceleration to avoid gradient disturbance. After centrifugation, tubes were fractionated in 12 density fractions that were weighed to check the gradient formation. DNA contained in each fraction was then precipitated using 2 volumes of polyethylene glycol (~0.8-1 mL), 1 µL glycogen (20 µg), centrifuged (13000g for 30 min) and washed with 70% purified ethanol (500 µL), and finally recovered in 30 µL TE buffer (10mM Tris-HCl and 1mM EDTA in deionized water) for further use.

On DNA recovered from each DNA fraction, the abundance of 16S rRNA genes was quantified using real-time quantitative PCR to determine the distribution of heavy and light DNA. Real-time PCR assays were performed in a 20 µL final volume, as previously described (Cebron et al., 2008) using: 2X iQ SYBR Green Supermix (Bio-Rad), 0.4 µmol.L^{-1} of each 16S rDNA universal primers 968F and 1401R (Nubel et al., 1996), BSA (0.06%), 0.2 µL DMSO (dimethylsulfoxyde), 0.08 µL t4gp32 protein (MP-Biomedicals) and 1 µL of DNA. The amplification was carried out with 40 cycles of four steps: 20 sec at 95°C, 20 sec at 56°C, and 30 sec at 72°C and 5 sec at 82°C (Cebron et al., 2008). On similar DNA fractions, fungal 18S rRNA genes were also quantified using real-time quantitative PCR (Thion et al., 2013) with the previously described primer pairs Fung5f-FF390r (Lueders et al., 2004), but no enrichment of

fungi was detected in heavy DNA fractions (Fig. S3) meaning that fungi were not significantly involved into PHE degradation because they did not incorporated ^{13}C in their DNA.

Identification of phenanthrene-degrading bacteria

Altogether, DNA from the 16 microcosm treatments (2 soil types, with and without rhamnolipids, at DT90, light and heavy DNA fractions n°3 and 7, from ^{12}C and ^{13}C incubations) and the two initial soils, in triplicate, were chosen for sequencing, resulting in 54 samples. Libraries of 16S rRNA gene amplicons were prepared for 454 pyrosequencing after amplification using universal primers 27F (5' – AGA GTT TGA TCC TGG CTC AG - 3') and 533R (5' – TTA CCG CGG CTG CTG GCA C - 3'), extended at the 5' end by 10 bp multiplex identifiers (MIDs, Roche). Amplifications were done with GoTaq G2 Green Master Mix (Promega). The amplification step was carried out with 25 and 30 cycles (30 sec at 95°C, 30 sec at 60°C, 30 sec at 72°C) for microcosm and initial soil samples, respectively. After quality checking on agarose gel electrophoresis and quantification using NanoDrop, three independent PCR products per sample were pooled together to minimize PCR bias on sequencing, and an equimolar mixture was then prepared. Pyrosequencing was carried out using a GS FLX 454 (Beckman Coulter Genomics, Danvers, MA, USA) and produced 316.5 megabases corresponding to a total of 716,250 partial 16S rRNA gene sequences having a median size of 490 bp. Sequence analyses, i.e. reducing sequencing error, removing chimeras, grouping into OTUs, subsampling to 1000 sequences, SILVA database alignment, and classifying using the RDP reference files were performed using MOTHUR (version 1.36), as recommended by its author (Schloss et al., 2011). Following the trimming, we obtained 250 bp sequences from the forward primer (corresponding to the V1 and V2 16S rDNA regions). The alpha diversity of the samples was estimated using the Chao1 richness estimator and the nonparametric Shannon diversity index considering a same number of sequences for each sample (i.e. 1000 sequences).

Statistical analyses

Statistical analyses (ANOVA, Student's t tests, Kruskall Wallis tests, Kolmogorov Smirnov tests), data analysis and Factorial Correspondence Analysis (FCA) on OTUs table, by using Bray-Curtis dissimilarity distance, were performed using XLStat software (version 2.01.16906, Addinsoft, Paris). Chao-1 and nonparametric Shannon diversity indexes were calculated on OTUs table, using MOTHUR (version 1.36). ADONIS tests were performed by using Bray-Curtis dissimilarity distance (R software, version 3.1.2, VEGAN package).

Nucleotide sequence accession numbers

All 16S rRNA gene sequences have been submitted to the NCBI Short Read Archive under the Bioproject accession number PRJNA312913.

Results

Physico-chemical properties of soils

Soil analyses show that the two soils were very different (Table 1), with the PPY soil characterized by acidic and moderate nutrient conditions and the Pv soil characterized by alkaline and higher nutrient availability. For both soils, the major grain size fraction was coarse silt, representing more than 40% dry weight of the mineral fraction (Table 1). Although both particle size distributions were close, by comparison with the Shepard diagram (Shepard, 1954), the PPY and the Pv soils correspond to sandy silt clayey and silt soils, respectively. Concerning the clayey fraction, total clay content was significantly higher ($P < 0.05$; Student's t test) in the Pv soil (20.2%) compared to the PPY (15.5%), but the nature of clays was different (Table 1).

For PPY soil, chlorites, illites and kaolinites (clays with the lower CEC, 10-40, 20-30 and 3-15 meq.g^{-1}, respectively; Morel, 1996) were dominant whereas smectites (80 meq.g^{-1} < CEC < 150 meq.g^{-1}) were dominant in the Pv soil. Consequently, the CEC of the Pv soil was higher than that of the PPY soil, especially due to clay types.

Concerning total organic carbon content (TOC), the PPY was the richest soil (Table 1). Residual carbon (RC) was dominant in both soils compared to pyrolysable carbon (PC), showing that OM tended to be mature and resistant to pyrolysis, and could potentially strongly sorb PHE. The main OM fraction in PPY soil corresponded to biomacromolecules whereas mature geomacromolecules, that are higher PHE sorbents, were dominant in the Pv soil.

Phenanthrene sorption and bioaccessibility

PHE sorption isotherms (Fig. 1) were similar for the PPY and the Pv soils (P > 0.05, Kolmogorov-Smirnov Test). In the low PHE concentration range, they can both be described by a linear partitioning model (R^2=0.965 and 0.981 for PPY and Pv soils, respectively) (Crampon et al., 2016). So K_d values were calculated from the slopes of the linear part of the sorption isotherms. The K_d partition coefficients were 718.7 L.kg^{-1} and 695.5 L.kg^{-1} for the PPY and the Pv soils, respectively. Water/organic carbon partition coefficients K_{oc} could be calculated from the K_d values and the total organic carbon fraction (f_{oc}), using the equation: $K_{oc}=K_d/f_{oc}$. Log K_{oc} values were 4.58 and 4.73 for PHE in the PPY and the Pv soils, respectively. Increases of PHE desorption and potentially of PHE bioaccessibility were observed for both soils when adding rhamnolipids in the aqueous medium (Fig. 1). Indeed, K_d values obtained in the presence of rhamnolipids were significantly lower (Student's t test, P < 0.05) than those obtained without biosurfactant: 206.2 L.kg^{-1} and 318.7 L.kg^{-1} for the PPY and the Pv soils, respectively (R^2=0.959 and 0.929 for PPY and Pv soils, respectively).

Phenanthrene dissipation kinetics

Although no marked lag phase was observed in our experimental conditions, PHE dissipation was slow at the beginning of the experiments. Only 20% of PHE was degraded during the first 8 and 20 days for the Pv and the PPY soils, respectively (Fig. 2). Then, PHE dissipation was faster in Pv soil compared to the PPY soil, as ca 90% of PHE was dissipated in 16 days in the Pv soil, while 42 days were necessary in the PPY soil. The same trends were observed in a previous experiment (Crampon et al., 2014), aiming, inter alia, to follow the degradation of 7 selected PAHs in different soils with the same sampling terms.

Kinetics of PHE dissipation in the presence of rhamnolipids did not show any significant impact of surfactant addition compared to the controls ($P > 0.05$, Student's t test; Fig. 2).

SIP experiment and ^{13}C labeled DNA isolation

Total community (^{12}C) and active ^{13}C-labeled PHE-degrading bacterial populations were studied at two incubation times corresponding to DT20 (time where 20% PHE is dissipated) and DT90 (time where 90% PHE is dissipated) for both soils: it corresponded to 8 and 16 days of incubation for the Pv soil and 20 and 42 days of incubation for the PPY soil (Fig. 2). For controls, DNA was analyzed from both ^{12}C and ^{13}C microcosms.

Quantitative PCR revealed a higher number of 16S rRNA gene copies in the lower densities (<1.70) of the CsCl gradient, corresponding to light DNA (that should contain only ^{12}C DNA) (Fig. 3). For further analyses the fraction n°3 (d = 1.689) was selected. Heavy DNA (that should contain all ^{13}C DNA) was recovered in the fractions with density ranging from 1.705 to 1.722 (Fig. 3). Higher numbers of 16S rRNA gene copies in these heavy fractions collected from the ^{13}C microcosms corresponded to the active ^{13}C-labeled PHE-degrading bacteria. For further analyses the fraction n°7 (d = 1.711) was selected. At DT20, the difference between the number of 16S rRNA gene copies in the fraction n°7 from ^{12}C and ^{13}C microcosms was only significant

366 for Pv soil microcosms ($P < 0.05$, ANOVA test; Fig. S2). In PPY soil microcosms, no ^{13}C
367 labeled DNA was detected at DT20. At DT90, significant differences ($P<0.05$, ANOVA test)
368 were observed between ^{12}C and ^{13}C microcosms, for both soils (Fig. 3). The amounts of 16S
369 rRNA gene copies in the heavy fraction of DNA were about 10 and 50 times higher for the ^{13}C
370 microcosms than for the ^{12}C microcosms for the PPY and the Pv soils, respectively. Therefore,
371 samples at DT90 were chosen for sequencing and analyzing the bacterial diversity. No
372 significant difference was observed in the level of ^{13}C incorporation between microcosms with
373 and without rhamnolipids (Fig. 3).
374 No significant difference in the number of fungal 18S rRNA gene copies was observed between
375 ^{12}C and ^{13}C microcosms (Fig. S3), meaning that ^{13}C from PHE was not used as a growth carbon
376 source by fungi.
377
378 **Characterization of bacterial communities and identification of PHE-degrading bacteria**
379 454-pyrosequencing was carried out on 54 soil samples, corresponding to the soils before
380 spiking and the fractions from the DNA-SIP experiment. After de-noising, a total of 211,519
381 16S rRNA gene sequences were obtained, with an average number of 3,917 sequences per
382 sample. Even if the rarefaction curves based on operational taxonomic units (OTUs; at 97%
383 identity) did not reach a plateau for the soils before spiking, the diversity corresponding to the
384 labeled ^{13}C DNA (*i.e.* PHE-degrading populations) seemed to be well sampled (Fig. S4).
385 Although species richness given by Chao1 index was slightly higher for the Pv soil
386 comparatively to the PPY soil, no significant differences ($P>0.05$, Kruskall-Wallis test) of alpha
387 diversity were observed between the two native soils (Table 2). Concerning the heavy fractions
388 from the ^{13}C microcosms (fractions PPY/Pv_13C_Rh+/-_H in Table 2), the observed richness
389 were lower than in the initial soil types or in controls, meaning that PHE-degrading bacteria
390 represent only a small fraction of the total community in both soils. This finding is more

391 pronounced for the Pv soil, meaning that a significantly smaller number of OTUs (P<0.05,
392 Kruskall-Wallis test) was involved in PHE degradation.
393 Factorial correspondence analysis (Fig. 4) was performed using the 100 most represented OTUs
394 (in each soil, separately) to highlight similarities and dissimilarities between replicates, sample
395 conditions (soil before spiking, ^{12}C and ^{13}C microcosms, or with and without rhamnolipids) and
396 DNA fractions (light and heavy). Whatever the soil type, the bacterial diversity retrieved from
397 the heavy DNA fractions of ^{13}C microcosms was significantly different from the diversity found
398 in the heavy DNA fractions of ^{12}C control microcosms (P<0.01; ADONIS test). A specific
399 analysis of the effect of rhamnolipids addition revealed no differences in each soil type between
400 treatments with and without rhamnolipids, in both light or heavy fractions (P>0.05; ADONIS
401 test). Notably, no differences appeared between the diversity in light DNA fractions from both
402 ^{12}C and ^{13}C microcosms and the diversity of soils before spiking.
403 The analysis of the sequence distribution in the OTUs represented in the heavy DNA fractions
404 from the ^{13}C labeled microcosms and having a significantly higher abundance than in the ^{12}C
405 control microcosms allowed us to identify the main ^{13}C-labeled PHE degrading bacteria (Table
406 3). Notably, this analysis revealed that the main PHE degraders identified were poorly
407 represented in the initial soils (from <0.01% to 0.29% of the total sequences, Table 3), as in the
408 light and heavy fractions of the ^{12}C microcosms (from <0.01% to 3.0% of the total sequences,
409 data not shown).
410 The six OTUs, representing the active PHE degraders in the Pv soil, were identified as members
411 of the *Betaproteobacteria* class, with a high proportion of the *Rhodocyclaceae* family and some
412 *Burkholderiales* (including the *Polaromonas* genus). Concerning the PPY soil, members of a
413 higher number of OTUs were involved in PHE degradation. The 13 OTUs representing the
414 active PHE degraders belonged to *Alpha-*, *Beta-*, *Gamma-Proteobacteria* and *Actinobacteria*.
415 Notably the OTUs Pv_PHE6 and PPY_PHE6 were both related to the *Polaromonas* genus

(Table 3), and appeared phylogenetically close (Fig. S5). Moreover, OTUs Pv_PHE4 and PPY_PHE12 corresponded to the same OTU affiliated to the *Rhodoferax* genus (Table 3 and Fig. S5).

The relative abundance of some PHE degraders increased or decreased depending on the presence or absence of rhamnolipids, but only in the case of some of the low abundance PHE degraders (Table 3). Notably, the proportion of the two OTUs related to the *Polaromonas* genus was significantly higher in the presence of rhamnolipids in both soils. By contrast, when rhamnolipids were added, the relative proportion of sequences related to the *Rhodoferax* genus was significantly higher for the PPY soil ($P < 0.05$), whereas it tended be lower for the Pv soil ($P > 0.05$). Altogether, our results revealed that direct addition of rhamnolipids to soil has a limited effect on the active PHE degrading bacteria.

Discussion

PHE accessibility was assessed by studying different physico-chemical properties of soil, and by characterizing PHE sorption isotherms with or without rhamnolipids. Overall, the two soils considered were characterized by a similar OM content, but a high variation in their clay contents and natures. While total organic carbon content was slightly higher in the PPY soil, OM was dominated by mature geomacromolecules in the Pv soil (Table 1). This fraction of OM combines constituents naturally stable or stabilized by physico-chemical processes, residues of fires and some anthropogenic pollutants like soot, *i.e.* black carbon (Sebag et al, 2006). The higher content of this more mature, carbonaceous and crystallized fraction in Pv soil make it probably more prone to a stronger PHE sorption than the PPY soil. The characterization of OM maturation state in soils is important because binding energies and sorption properties towards PAHs increase over time (Ran et al., 2007). Indeed, PAHs sorption is generally lower and more reversible on fresh OM compared to aged OM because with ageing, the polar mixtures of

441 biomolecules transforms into a more hydrophobic form with higher sorptive properties for
442 lipophilic organic compounds (Mechlińska et al., 2009). Moreover, both total clay contents and
443 natures varied significantly between the two soil types considered. Chlorites, illites and
444 kaolinites were dominant in the PPY soil, whereas smectite was dominant in the Pv soil.
445 Although clay is generally described as a parameter affecting less PAH sorption to soil particles
446 compared to organic matter, it has to be considered here because of the potential impact on
447 rhamnolipids (Delle Site, 2001; Hwang and Cutright, 2002). Indeed, it has been reported that
448 sorption of rhamnolipids to soil is more strongly influenced by clay contents and nature than
449 by OM : at low biosurfactant concentrations, that are relevant for enhancing organic
450 contaminant biodegradation, clays and particularly kaolinite are the strongest sorbents for
451 rhamnolipids (Ochoa-Loza et al., 2007). So clays could influence observed results on PHE
452 remobilization.
453 Interestingly, despite these different physico-chemical properties and biodegradation kinetics,
454 PHE sorption was found to be quite similar in the two soil types. These results are consistent
455 with a previous study, where we showed that the bioaccessible fraction of PHE, estimated using
456 a mild extraction method (extraction with hydroxypropyl-β-cyclodextrin) was close between
457 these two soil types (Crampon et al., 2014). Furthermore, rhamnolipids addition increased PHE
458 desorption in both soil types, but with a greater effect in the PPY soil. Although no consensus
459 exists on the real positive or negative effect of rhamnolipids on PAH removal, several studies
460 reported a strong impact of soil organic matter content and contamination ageing (Congiu and
461 Ortega-Calvo, 2014; Szulc et al., 2014). Thus, the lowest PHE desorption from the Pv soil by
462 rhamnolipids addition could be explained by higher contents of mature OM, smectites and
463 kaolinite in the Pv soil. These soil constituents may enhance the formation of clay-humic
464 complexes and thus contribute to a strong adsorption of PHE on these complexes. Moreover,
465 these clay minerals increase the surface available for PAH as well as rhamnolipids sorption.

466 The presence of higher contents of kaolinite in Pv soil (Table 1) can explain the strongest
467 sorption of the biosurfactant on Pv soil, compared to PPY soil. Consequently, there may be less
468 micelles in the soil solution to remobilize PHE and more additional sorption sites through
469 rhamnolipids sorbed on soil aggregates (Ochoa-Loza et al., 2007; Zhou and Zhu, 2007).
470 Although rhamnolipids significantly increased PHE desorption in the two soil types tested,
471 addition of a biosurfactant had a limited impact on the PAH biodegradation efficiency (Fig. 2).
472 While some studies report that surfactants may increase PAH biodegradation rates, others have
473 shown that the effect of their application may be negligible (Laha and Luthy, 1991; Rouse et
474 al., 1994; Tiehm, 1994; Tsomides et al., 1995). Indeed, Leonardi *et al*. (Leonardi et al., 2007)
475 showed that when a soil is characterized by a low non-bioaccessible PAH fraction, addition of
476 surfactant has a limited impact on the PAH biodegradation efficiency. Moreover, the effect of
477 the surfactant could also depend on the identity of PAH-degrading bacteria involved (Allen et
478 al., 1999). At last, we can also suppose that if rhamnolipids can partially desorb PAHs from
479 soils, they can also desorb them from the surface of bacteria, which can lead to the decrease of
480 their bioavailability while they increase their bioaccessibility.
481 More generally, other factors might explain the difference in degradation rate observed between
482 the two soils. Indeed, the optimum pH range can be very variable depending on the type of soil
483 and the PAH-degrading bacteria (Simarro et al., 2011). It could not be excluded that the basic
484 Pv soil allowed a greater activity of the PAH-degrading bacteria than the acidic PPY soil.
485 Moreover, difference in initial concentrations of nitrogen and carbon between the two soils may
486 also affect the activity of the PAH-degrading bacteria (Teng et al., 2010). Temperature and
487 toxicity of PAHs could also impact the biodegradation rate (Coover and Sims, 1987; Martin et
488 al., 2012). Indeed, native high molecular weight PAHs (4-6 ring PAHs), which can be
489 considered as the most toxic PAHs, were 2.5 times more concentrated in Pv soil than in PPY
490 soil. However, it must be noted that they represent only 0.09-0.22% of the total amount of PAHs

491 after PHE spiking, which is quite negligible. Interestingly, all the factors having a potential
492 impact on the PHE degradation kinetics have in common to influence the physiology of the
493 PAH-degrading bacteria.
494 In a second phase, we therefore studied the diversity of the PAH-degrading bacteria in order (i)
495 to compare the PAH-degrading populations between these two soils and (ii) to evaluate the
496 impact of a bioavailability variation on these degrading populations. The combination of ^{13}C
497 labeled PHE and 16S rRNA gene amplicon pyrosequencing enabled us to identify the PHE-
498 degrading bacterial communities in these two contrasted soil types.
499 Most of the PHE degraders identified in the two soil types belonged to the *Proteobacteria*
500 phylum. Some members of the *Alphaproteobacteria* (Demaneche et al., 2004),
501 *Betaproteobacteria* (Goyal and Zylstra, 1997; Laurie and Lloyd-Jones, 1999; Seo et al., 2009)
502 and *Gammaproteobacteria* (Balashova et al., 2001; Ensley et al., 1982; Kiyohara et al., 1994;
503 Resnick and Gibson, 1996) classes possess specific PAH dioxygenases involved in the catalysis
504 of the initial aromatic ring oxidation (Cebron et al., 2008; Habe and Omori, 2003). Some OTUs
505 belonging to these classes were found among PHE degraders in the PPY soil. In addition, one
506 OTU of the PHE degraders belongs to the *Mycobacterium* genera (*Actinobacteria*) that has
507 already been described as a good PAH degrader in soils (Timmis et al., 2010). Altogether, these
508 PHE degraders were poorly represented in both initial soil bacterial communities, indicating
509 that when soil PAH are diffusely concentrated, the PHE-degraders belong to the rare biosphere,
510 but could rapidly become active when available PAHs enter the system.
511 The Pv soil presented a lower diversity of PHE degraders than the PPY soil, all belonging to
512 the *Betaproteobacteria*. It was further shown that the abundance of *Betaproteobacteria*
513 increased after three months of incubation in microcosms spiked with PHE, pyrene or a mix of
514 seven PAHs, members of this bacterial class being largely described as capable of degrading
515 PAHs (Jeon et al., 2003; Martin et al., 2012; Niepceron et al., 2013; Núñez et al., 2012;

Singleton et al., 2006). Among the *Betaproteobacteria* class, sequences related to members of the *Rhodocyclaceae* family were the most represented in the ^{13}C fraction (more than 80% of the sequences), suggesting a major role in PHE degradation in the Pv soil. Interestingly, representatives of these taxa have also been described as able to degrade PAHs and to possess specific PAH RHD enzymes (Chemerys et al., 2014; Martin et al., 2012; Regonne et al., 2013; Singleton et al., 2006; Uhlik et al., 2012), and a cultivable member of this *Rhodocyclaceae* family that degrades PAHs has been recently sequenced (Singleton et al., 2015). The exceptional PAH degradation capacity of *Rhodocyclaceae* in various soils suggests classifying them as very efficient PHE degraders. Since previous representatives of this taxon have already been shown to efficiently degrade PAHs (Singleton et al., 2015), the *Rhodocyclaceae* family may be used as a bioindicator of soils with a high PHE degradation capacity. Moreover, cultivation-dependent analysis combined to genome sequencing should permit to further understand the functional role of the *Rhodocyclaceae* family in PAH degradation.

Interestingly, the diversity and the structure of the main PHE degraders seem only slightly impacted by rhamnolipids addition and no impact on the total bacterial community was detected. Such results suggest that the rhamnolipid amendment used in biostimulation processes is probably not used as carbon source, and may be a good alternative in term of toxicity for the soil bacterial communities compared to synthetic surfactants. However, its use for soils where bioaccessibility is not a limiting degradation parameter does not seem to be an advantage even if it improved PHE desorption in both soils.

Conclusion

By using chemical and microbiological methods, we demonstrated that the PHE bioaccessibility has a low impact on its degradation. Indeed, the difference in biodegradation rates we found between the two soils considered cannot be explained by a difference in

bioaccessibility. Moreover, although the amendment of biosurfactants (*i.e.* rhamnolipids) did change the PHE sorption/desorption kinetics in the two soils tested, no significant impact on PHE degradation rates was detected. In addition, we showed that variation in biodegradation rate between these diffusely contaminated soils could be more explained by the differences in PHE-degrading populations, which presence and activities might be driven by physico-chemical properties of the soils. Finally, we showed, for the first time to our knowledge, that rhamnolipids present a low toxicity for soil microorganisms as they do not modify the global bacterial diversity as well as the activity of the phenanthrene-degraders. In the future, it could be interesting to investigate the degradation kinetics of a mixture of PAHs (e.g. the 16 priority PAHs) with or without rhamnolipids and to identify the bacteria more particularly involved in the degradation of heavy high molecular weight PAHs.

Acknowledgements

The authors thank the "Région Haute Normandie" (France) for financial support through the Normandy SCALE research network (RESSOLV program). The authors thank the Ecogenomic plateform (INRA Nancy, France) for the using of the ultracentrifuge. The authors thank Jennifer Hellal for her help in proofreading the paper.

Supporting information

Five Figures (Figure S1, S2, S3, S4 and S5) are included in the supporting information.

References

Ahangar, A.G., 2010. Sorption of PAHs in the soil environment with emphasis on the role of soil organic matter: A review. World Applied Sciences Journal 11, 759-765.

565 Ahn, C.K., Kim, Y.M., Woo, S.H., Park, J.M., 2008. Soil washing using various nonionic
566 surfactants and their recovery by selective adsorption with activated carbon. Journal of
567 Hazardous Matererials 154, 153-160.
568 Allen, C.C.R., Boyd, D.R., Hempenstall, F., Larkin, M.J., Sharma, N.D., 1999. Contrasting
569 effects of a nonionic surfactant on the biotransformation of polycyclic aromatic
570 hydrocarbons tocis-dihydrodiols by soil bacteria. Applied and Environmental Microbiology
571 65, 1335-1339.
572 Balashova, N., Stolz, A., Knackmuss, H., Kosheleva, I., Naumov, A., Boronin, A., 2001.
573 Purification and characterization of a salicylate hydroxylase involved in 1-hydroxy-2-
574 naphthoic acid hydroxylation from the naphthalene and phenanthrene-degrading bacterial
575 strain *Pseudomonas putida* BS202-P1. Biodegradation 12, 179-188.
576 Barnier, C., Ouvrard, S., Robin, C., Morel, J.L., 2014. Desorption kinetics of PAHs from aged
577 industrial soils for availability assessment. Science of the Total Environment 470, 639-645.
578 Bordas, F., Lafrance, P., Villemur, R., 2005. Conditions for effective removal of pyrene from
579 an artificially contaminated soil using *Pseudomonas aeruginosa* 57SJ rhamnolipids.
580 Environmental Pollution 138, 69-76.
581 Brandli, R.C., Hartnik, T., Henriksen, T., Cornelissen, G., 2008. Sorption of native
582 polyaromatic hydrocarbons (PAH) to black carbon and amended activated carbon in soil.
583 Chemosphere 73, 1805-1810.
584 Bustamante, M., Durán, N., Diez, M.C., 2012. Biosurfactants are useful tools for the
585 bioremediation of contaminated soil: a review. Journal of Soil Science and Plant Nutrition
586 12, 667-687.
587 Cebron, A., Norini, M.P., Beguiristain, T., Leyval, C., 2008. Real-Time PCR quantification of
588 PAH-ring hydroxylating dioxygenase (PAH-RHDalpha) genes from Gram positive and

589 Gram negative bacteria in soil and sediment samples. Journal of Microbiological Methods
590 73, 148-159.
591 Chemerys, A., Pelletier, E., Cruaud, C., Martin, F., Violet, F., Jouanneau, Y., 2014.
592 Characterization of novel polycyclic aromatic hydrocarbon dioxygenases from the bacterial
593 metagenomic DNA of a contaminated soil. Applied and Environmental Microbiology 80,
594 6591-6600.
595 Congiu, E., Ortega-Calvo, J.-J., 2014. Role of desorption kinetics in the rhamnolipid-enhanced
596 biodegradation of polycyclic aromatic hydrocarbons. Environmental Science & Technology
597 48, 10869-10877.
598 Coover, M.P., Sims, R.C., 1987. The effect of temperature on polycyclic aromatic hydrocarbon
599 persistence in an unacclimated agricultural soil. Hazardous Waste and Hazardous Materials
600 4, 69-82.
601 Crampon, M., Bureau, F., Akpa-Vinceslas, M., Bodilis, J., Machour, N., Le Derf, F., Portet-
602 Koltalo, F., 2014. Correlations between PAH bioavailability, degrading bacteria, and soil
603 characteristics during PAH biodegradation in five diffusely contaminated dissimilar soils.
604 Environmental Science and Pollution Research 21, 8133-8145.
605 Crampon, M., Bodilis, J., Le Derf, F., Portet-Koltalo, F., 2016. Alternative techniques to HPCD
606 to evaluate the bioaccessible fraction of soil-associated PAHs and correlation to
607 biodegradation efficiency. Journal of Hazardous Materials 314, 220-229
608 Delle Site, A., 2001. Factors affecting sorption of organic compounds in natural sorbent/water
609 systems and sorption coefficients for selected pollutants. A Review. Journal of Physical and
610 Chemical Reference Data 30, 187-439.
611 Demaneche, S., Meyer, C., Micoud, J., Louwagie, M., Willison, J.C., Jouanneau, Y., 2004.
612 Identification and functional analysis of two aromatic-ring-hydroxylating dioxygenases

613 from a *Sphingomonas* strain that degrades various polycyclic aromatic hydrocarbons.
614 Applied and Environmental Microbiology 70, 6714-6725.
615 Doyle, E., Muckian, L., Hickey, A.M., Clipson, N., 2008. Microbial PAH degradation.
616 Advances in Applied Microbiology 65, 27-66.
617 Ensley, B.D., Gibson, D.T., Laborde, A.L., 1982. Oxidation of naphthalene by a
618 multicomponent enzyme system from *Pseudomonas* sp. strain NCIB 9816. Journal of
619 Bacteriology 149, 948-954.
620 Goyal, A., Zylstra, G., 1997. Genetics of naphthalene and phenanthrene degradation by
621 *Comamonas testosteroni*. Journal of Industrial Microbiology and Biotechnology 19, 401-
622 407.
623 Groboillot, A., Portet-Koltalo, F., Le Derf, F., Feuilloley, M.J., Orange, N., Poc, C.D., 2011.
624 Novel application of cyclolipopeptide amphisin: feasibility study as additive to remediate
625 polycyclic aromatic hydrocarbon (PAH) contaminated sediments. International Journal of
626 Molecular Science 12, 1787-1806.
627 Habe, H., Omori, T., 2003. Genetics of polycyclic aromatic hydrocarbon metabolism in diverse
628 aerobic bacteria. Bioscience, Biotechnology, and Biochemistry 67, 225-243.
629 Haritash, A., Kaushik, C., 2009. Biodegradation aspects of polycyclic aromatic hydrocarbons
630 (PAHs): a review. Journal of Hazardous Materials 169, 1-15.
631 Hwang, S., Cutright, T.J., 2002. Impact of clay minerals and DOM on the competitive
632 sorption/desorption of PAHs. Soil and Sediment Contamination: An International Journal
633 11, 269-291.
634 Jeon, C.O., Park, M., Ro, H.-S., Park, W., Madsen, E.L., 2006. The naphthalene catabolic (*nag*)
635 genes of *Polaromonas naphthalenivorans* CJ2: evolutionary implications for two gene
636 clusters and novel regulatory control. Applied and Environmental Microbiology 72, 1086-
637 1095.

638 Jeon, C.O., Park, W., Padmanabhan, P., DeRito, C., Snape, J.R., Madsen, E.L., 2003. Discovery
639 of a bacterium, with distinctive dioxygenase, that is responsible for *in situ* biodegradation in
640 contaminated sediment. Proceedings of the National Academy of Sciences 100, 13591-
641 13596.
642 Jonker, M.T., Hawthorne, S.B., Koelmans, A.A., 2005. Extremely slowly desorbing polycyclic
643 aromatic hydrocarbons from soot and soot-like materials: evidence by supercritical fluid
644 extraction. Environmental Science & Technology 39, 7889-7895.
645 Kim, J.M., Jeon, C.O., 2009. Isolation and characterization of a new benzene, toluene, and
646 ethylbenzene degrading bacterium, *Acinetobacter sp.* B113. Current Microbiology 58, 70-
647 75.
648 Kiyohara, H., Torigoe, S., Kaida, N., Asaki, T., Iida, T., Hayashi, H., Takizawa, N., 1994.
649 Cloning and characterization of a chromosomal gene cluster, *pah*, that encodes the upper
650 pathway for phenanthrene and naphthalene utilization by *Pseudomonas putida* OUS82.
651 Journal of Bacteriology 176, 2439-2443.
652 Laha, S., Luthy, R.G., 1991. Inhibition of phenanthrene mineralization by nonionic surfactants
653 in soil-water systems. Environmental science & technology 25, 1920-1930.
654 Laurie, A.D., Lloyd-Jones, G., 1999. The *phn* genes of *Burkholderia sp.* strain RP007 constitute
655 a divergent gene cluster for polycyclic aromatic hydrocarbon catabolism. Journal of
656 Bacteriology 181, 531-540.
657 Leonardi, V., Šašek, V., Petruccioli, M., D'Annibale, A., Erbanová, P., Cajthaml, T., 2007.
658 Bioavailability modification and fungal biodegradation of PAHs in aged industrial soils.
659 International Biodeterioration & Biodegradation 60, 165-170.
660 Lueders, T., Wagner, B., Claus, P., Friedrich, M.W., 2004. Stable isotope probing of rRNA and
661 DNA reveals a dynamic methylotroph community and trophic interactions with fungi and
662 protozoa in oxic rice field soil. Environmental Microbiology 6, 60-72.

663 Martin, F., Torelli, S., Le Paslier, D., Barbance, A., Martin-Laurent, F., Bru, D., Geremia, R.,
664 Blake, G., Jouanneau, Y., 2012. *Betaproteobacteria* dominance and diversity shifts in the
665 bacterial community of a PAH-contaminated soil exposed to phenanthrene. Environmental
666 Pollution 162, 345-353.
667 Mechlińska, A., Gdaniec-Pietryka, M., Wolska, L., Namieśnik, J., 2009. Evolution of models
668 for sorption of PAHs and PCBs on geosorbents. TrAC Trends in Analytical Chemistry 28,
669 466-482.
670 Neufeld, J.D., Vohra, J., Dumont, M.G., Lueders, T., Manefield, M., Friedrich, M.W., Murrell,
671 J.C., 2007. DNA stable-isotope probing. Nature Protocols 2, 860-866.
672 Niepceron, M., Martin-Laurent, F., Crampon, M., Portet-Koltalo, F., Akpa-Vinceslas, M.,
673 Legras, M., Bru, D., Bureau, F., Bodilis, J., 2013. *GammaProteobacteria* as a potential
674 bioindicator of a multiple contamination by polycyclic aromatic hydrocarbons (PAHs) in
675 agricultural soils. Environmental Pollution 180, 199-205.
676 Nubel, U., Engelen, B., Felske, A., Snaidr, J., Wieshuber, A., Amann, R.I., Ludwig, W.,
677 Backhaus, H., 1996. Sequence heterogeneities of genes encoding 16S rRNAs in
678 *Paenibacillus polymyxa* detected by temperature gradient gel electrophoresis. Journal of
679 Bacteriology 178, 5636-5643.
680 Núñez, E.V., Valenzuela-Encinas, C., Alcántara-Hernández, R.J., Navarro-Noya, Y.E., Luna-
681 Guido, M., Marsch, R., Dendooven, L., 2012. Modifications of bacterial populations in
682 anthracene contaminated soil. Applied Soil Ecology 61, 113-126.
683 Ochoa-Loza, F.J., Noordman, W.H., Jannsen, D.B., Brusseau, M.L., Maier, R.M., 2007. Effect
684 of clays, metal oxides, and organic matter on rhamnolipid biosurfactant sorption by soil.
685 Chemosphere 66, 1634-1642.
686 Paria, S., 2008. Surfactant-enhanced remediation of organic contaminated soil and water.
687 Advances in Colloid and Interface Science 138, 24-58.

688 Portet-Koltalo, F., Ammami, M.T., Benamar, A., Wang, H., Le Derf, F., Duclairoir-Poc, C.,
689 2013. Investigation of the release of PAHs from artificially contaminated sediments using
690 cyclolipopeptidic biosurfactants. Journal of Hazardous Materials 261, 593-601.
691 Portet-Koltalo, F., Oukebdane, K., Dionnet, F., Desbène, P., 2008. Optimisation of the
692 extraction of polycyclic aromatic hydrocarbons and their nitrated derivatives from diesel
693 particulate matter using microwave-assisted extraction. Analytical and Bioanalytical
694 Chemistry 390, 389-398.
695 Ran, Y., Sun, K., Ma, X., Wang, G., Grathwohl, P., Zeng, E.Y., 2007. Effect of condensed
696 organic matter on solvent extraction and aqueous leaching of polycyclic aromatic
697 hydrocarbons in soils and sediments. Environmental Pollution 148, 529-538.
698 Regonne, R.K., Martin, F., Mbawala, A., Ngassoum, M.B., Jouanneau, Y., 2013. Identification
699 of soil bacteria able to degrade phenanthrene bound to a hydrophobic sorbent *in situ*.
700 Environmental Pollution 180, 145-151.
701 Resnick, S.M., Gibson, D.T., 1996. Regio-and stereospecific oxidation of fluorene,
702 dibenzofuran, and dibenzothiophene by naphthalene dioxygenase from *Pseudomonas sp.*
703 strain NCIB 9816-4. Applied and Environmental Microbiology 62, 4073-4080.
704 Riding, M.J., Doick, K.J., Martin, F.L., Jones, K.C., Semple, K.T., 2013. Chemical measures
705 of bioavailability/bioaccessibility of PAHs in soil: fundamentals to application. Journal of
706 Hazardous Materials 261, 687-700.
707 Rouse, J.D., Sabatini, D.A., Suflita, J.M., Harwell, J.H., 1994. Influence of surfactants on
708 microbial degradation of organic compounds. Critical Reviews in Environmental Science
709 and Technology 24, 325-370.
710 Schloss, P.D., Gevers, D., Westcott, S.L., 2011. Reducing the effects of PCR amplification and
711 sequencing artifacts on 16S rRNA-based studies. PloS one 6, e27310.

712 Sebag, D., Disnar, J.R., Guillet, B., Di Giovanni, C., Verrecchia, E.P., Durand, A., 2006.
713 Monitoring organic matter dynamics in soil profiles by 'Rock-Eval pyrolysis': bulk
714 characterization and quantification of degradation. European Journal of Soil Science 57,
715 344-355.
716 Semple, K.T., Doick, K.J., Jones, K.C., Burauel, P., Craven, A., Harms, H., 2004. Peer
717 reviewed: defining bioavailability and bioaccessibility of contaminated soil and sediment is
718 complicated. Environmental Science & Technology 38, 228A-231A.
719 Semple, K.T., Morriss, A.W.J., Paton, G.I., 2003. Bioavailability of hydrophobic organic
720 contaminants in soils: fundamental concepts and techniques for analysis. European Journal
721 of Soil Science 54, 809-818.
722 Seo, J.S., Keum, Y.S., Li, Q.X., 2009. Bacterial degradation of aromatic compounds.
723 International Journal of Environmental Research and Public Health 6, 278-309.
724 Shepard, F.P., 1954. Nomenclature based on sand-silt-clay ratios. Journal of Sedimentary
725 Research 24.
726 Simarro, R., Gonzalez, N., Bautista, L. F., Sanz, R., and Molina, M. C., 2011. Optimisation of
727 key abiotic factors of PAH (naphthalene, phenanthrene, and anthracene) biodegradation
728 process by a bacterial consortium. Water, Air, & Soil Pollution 217, 365–374.
729 Singleton, D.R., Dickey, A.N., Scholl, E.H., Wright, F.A., Aitken, M.D., 2015. Complete
730 genome sequence of a novel bacterium within the family *Rhodocyclaceae* that degrades
731 polycyclic aromatic hydrocarbons. Genome Announcements 3, e00251-00215.
732 Singleton, D.R., Sangaiah, R., Gold, A., Ball, L.M., Aitken, M.D., 2006. Identification and
733 quantification of uncultivated *Proteobacteria* associated with pyrene degradation in a
734 bioreactor treating PAH-contaminated soil. Environmental Microbiology 8, 1736-1745.
735 Szulc, A., Ambrożewicz, D., Sydow, M., Ławniczak, Ł., Piotrowska-Cyplik, A., Marecik, R.,
736 Chrzanowski, Ł., 2014. The influence of bioaugmentation and biosurfactant addition on

737 bioremediation efficiency of diesel-oil contaminated soil: Feasibility during field studies.
738 Journal of Environmental Management 132, 121-128.
739 Teng, Y., Luo, Y., Ping, L., Zou, D., Li, Z., Christie, P., 2010. Effects of soil amendment with
740 different carbon sources and other factors on the bioremediation of an aged PAH-
741 contaminated soil. Biodegradation 21, 167–78.
742 Thion, C., Cébron, A., Beguiristain, T., Leyval, C., 2013. Inoculation of PAH-degrading strains
743 of *Fusarium solani* and *Arthrobacter* oxydans in rhizospheric sand and soil microcosms:
744 microbial interactions and PAH dissipation. Biodegradation 24, 569-581.
745 Tiehm, A., 1994. Degradation of polycyclic aromatic hydrocarbons in the presence of synthetic
746 surfactants. Applied and Environmental Microbiology 60, 258-263.
747 Timmis, K.N., McGenity, T., Van Der Meer, J., De Lorenzo, V., 2010. Handbook of
748 hydrocarbon and lipid microbiology. Springer Berlin.
749 Tobiszewski, M., Namieśnik, J., 2012. PAH diagnostic ratios for the identification of pollution
750 emission sources. Environmental Pollution 162, 110-119.
751 Tsomides, H.J., Hughes, J.B., Thomas, J.M., Ward, C.H., 1995. Effect of surfactant addition on
752 phenanthrene biodegradation in sediments. Environmental Toxicology and Chemistry 14,
753 953-959.
754 Uhlik, O., Wald, J., Strejcek, M., Musilova, L., Ridl, J., Hroudova, M., Vlcek, C., Cardenas, E.,
755 Mackova, M., Macek, T., 2012. Identification of bacteria utilizing biphenyl, benzoate, and
756 naphthalene in long-term contaminated soil. PloS one 7, e40653.
757 Wu, Y., Luo, Y., Zou, D., Ni, J., Liu, W., Teng, Y., Li, Z., 2008. Bioremediation of polycyclic
758 aromatic hydrocarbons contaminated soil with *Monilinia sp.*: degradation and microbial
759 community analysis. Biodegradation 19, 247-257.
760 Xia, X., Li, Y., Zhou, Z., Feng, C., 2010. Bioavailability of adsorbed phenanthrene by black
761 carbon and multi-walled carbon nanotubes to *Agrobacterium*. Chemosphere 78, 1329-1336.

762 Zhou, J., Jiang, W., Ding, J., Zhang, X., Gao, S., 2007. Effect of Tween 80 and β-cyclodextrin
763 on degradation of decabromodiphenyl ether (BDE-209) by White Rot Fungi. Chemosphere
764 70, 172-177.
765 Zhou, W., Zhu, L., 2007. Efficiency of surfactant-enhanced desorption for contaminated soils
766 depending on the component characteristics of soil-surfactant–PAHs system. Environmental
767 Pollution 147, 66-73.
768 Zhou, W., Zhu, L., 2008. Enhanced soil flushing of phenanthrene by anionic–nonionic mixed
769 surfactant. Water Research 42, 101-108.
770

771 TABLE 1: Physico-chemical properties of the two studied soils (Pv and PPY).

Method	Data	PPY	Pv
Granulometry without decarbonatation (% dry weight)	*Clays (<2µm)*	15.5	20.2
	Fine silts (2 < D < 20 µm)	23.4	26.0
	Coarse silts (20 < D < 50 µm)	42.3	44.2
	Fine sands (50 < D < 200 µm)	17.8	9.5
	Coarse sands (200 < D < 2000 µm)	1.0	0.1
XRD (g.kg^{-1})	*Chlorite*	36.5	0.0
	Illite / Chlorite	11.2	0.0
	Illite	53.7	44.8
	Kaolinite	53.6	66.8
	Smectite	0.0	90.4
RockEval6 Pyrolysis & S2 peak deconvolution [a] (g.kg^{-1})	*Total Organic Carbon (TOC)*	18.7	13.1
	Pyrolysable carbon (PC)	4.2	2.6
	Residual carbon (RC)	14.5	10.6
	Biomacromolecules	8.2	4.5
	Immature geomacromolecules	5.4	2.4
	Mature geomacromolecules	5.1	6.2
pH (H_2O)		5.7	8.2
Cationic Exchange Capacity CEC (cmol.kg^{-1})		8.7	14.2
PAHs (mg.kg^{-1}) (n=6)	*16 PAHs (US-EPA)*	0.320 ± 0.040	0.890 ± 0.290
	BaP	0.019 ± 0.006	0.046 ± 0.022
	PHE	0.035 ± 0.012	0.013 ± 0.001

772

773 [a] *The deconvolution of S2 peak, which can be related to soil OM (cracking between 200 to*

774 *650 °C), allowed a precise determination of the maturation of OM in soils.*

775

776

TABLE 2: Alpha diversity indexes of the two studied soils (Pv and PPY) based on OTUs formed at 97% similarity.

Samples[b]	0.03[c]		
	OTU	Chao1	H'
Pv[d, x]	446 ± 105	1194 ± 139	6.19 ± 0.33
Pv_12C_Rh+_L[x]	417 ± 64	1031 ± 124	5.75 ± 0.42
Pv_12C_Rh+_H[x]	376 ± 59	840 ± 114	5.34 ± 0.59
Pv_12C_Rh-_L[x]	411 ± 135	965 ± 356	5.75 ± 0.67
Pv_12C_Rh-_H[x]	423 ± 148	1000 ± 348	5.76 ± 0.82
Pv_13C_Rh+_L[x]	417 ± 12	1028 ± 48	5.78 ± 0.04
Pv_13C_Rh+_H[y]	54 ± 1	195 ± 16	1.72 ± 0.06
Pv_13C_Rh-_L[x]	452 ± 6	1143 ± 59	5.94 ± 0.04
Pv_13C_Rh-_H[y]	40 ± 3	137 ± 28	1.62 ± 0.19
PPY[d, x]	413 ± 20	880 ± 61	5.82 ± 0.09
PPY_12C_Rh+_L[x]	310 ± 61	632 ± 123	5.17 ± 0.57
PPY_12C_Rh+_H[x]	334 ± 107	668 ± 220	5.25 ± 0.70
PPY_12C_Rh-_L[x]	347 ± 31	741 ± 82	5.45 ± 0.19
PPY_12C_Rh-_H	319 ± *NA*[e]	597 ± *NA*[e]	5.04 ± *NA*[e]
PPY_13C_Rh+_L[x]	347 ± 4	738 ± 23	5.47 ± 0.02
PPY_13C_Rh+_H[z]	171 ± 59	406 ± 136	3.65 ± 0.92
PPY_13C_Rh-_L[x]	335 ± 61	710 ± 122	5.34 ± 0.47
PPY_13C_Rh-_H[z]	241 ± 67	609 ± 189	4.22 ± 0.56

[a] x, y and z represent the different groups characterized statistically ($p<0.05$, Kruskall Wallis test)
[b] $Rh^{+/-}$: with or without rhamnolipid addition; L/H: light or heavy DNA fractions.
[c] 0.03 is the OTU cutoff in distance units, OTU means the number of OTUs observed, Chao1 means the Chao1 estimated minimum number of OTUs and H′ means the nonparametric Shannon diversity index.
[d] Soil before spiking
[e] Not Applicable, for samples with not enough reads for calculation of standard deviation with triplicates.

785 TABLE 3: Active ^{13}C-labeled PHE degraders in the two studied soils (Pv and PPY). OTUs
786 were considered as PHE-degraders when a significantly higher proportion was recovered in
787 heavy DNA fractions from ^{13}C microcosms than from ^{12}C microcosms.

Soil	OTU	Taxonomic identification		Relative abundance of this OTU found (%)		
		Phylum / Class	Best resolution[a]	With Rhamnolipids	Without Rhamnolipids	Native soil
Pv	*Pv_PHE1*	Betaproteobacteria	Rhodocyclacae family	52.48 ± 2.91	50.06 ± 11.22	0.01 ± 0.01
	Pv_PHE2	Betaproteobacteria	Rhodocyclacae family	19.77 ± 1.44	17.95 ± 3.9	<0.01
	Pv_PHE3	Betaproteobacteria	Rhodocyclacae family	15.69 ± 2.02	13.69 ± 2.42	<0.01
	Pv_PHE4[b]	Betaproteobacteria	*Rhodoferax*	3.16 ± 2.9	12.02 ± 8.28	0.12 ± 0.05
	Pv_PHE5	Betaproteobacteria	*Hydrogenophaga*	0.76 ± 0.08	1.11 ± 1.3	0.03 ± 0.04
	Pv_PHE6[c]	Betaproteobacteria	*Polaromonas*	0.89 ± 0.44	0.15 ± 0.13	0.02 ± 0.03
PPY	*PPY_PHE1*	Gammaproteobacteria	*Nevskia*	23.90 ± 18.53	23.92 ± 11.07	<0.01
	PPY_PHE2	Betaproteobacteria	Burkholderiales order	11.61 ± 10.5	6.31 ± 2.57	0.01 ± 0.02
	PPY_PHE3	Betaproteobacteria	*Collimonas*	2.13 ± 0.82	7.89 ± 6.53	0.29 ± 0.2
	PPY_PHE4	Alphaproteobacteria	Hyphomicrobiaceae family	6.22 ± 3.91	2.55 ± 1.09	0.25 ± 0.12
	PPY_PHE5	Gammaproteobacteria	*Dyella*	4.86 ± 2.53	3.53 ± 2.57	0.04 ± 0.03
	PPY_PHE6[c]	Betaproteobacteria	*Polaromonas*	6.59 ± 4.59	1.11 ± 0.22	<0.01
	PPY_PHE7	Alphaproteobacteria	Hyphomicrobiaceae family	2.30 ± 0.9	3.12 ± 3.83	0.03 ± 0.06
	PPY_PHE8	Gammaproteobacteria	*Nevskia*	0.91 ± 0.55	1.60 ± 2.24	<0.01
	PPY_PHE9	Alphaproteobacteria	Acetobacteraceae family	1.51 ± 0.47	1.49 ± 1.19	<0.01
	PPY_PHE10	Actinobacteria	*Mycobacterium*	2.04 ± 1.96	0.73 ± 0.46	<0.01
	PPY_PHE11	Betaproteobacteria	*Herbaspirillum*	0.93 ± 1.20	1.17 ± 0.76	<0.01
	PPY_PHE12[b, c]	Betaproteobacteria	*Rhodoferax*	1.40 ± 0.15	0.37 ± 0.64	0.10 ± 0.09
	PPY_PHE13	Gammaproteobacteria	*Nevskia*	0.46 ± 0.46	1.21 ± 1.52	<0.01

788 [a] These taxonomic identifications were confirmed phylogenetically (FIG S5)

789 [b] The two OTUs Pv_PHE4 and PPY_PHE12 are similar
790 [c] These OTUs showed significant difference between microcosms with and without rhamnolipids ($P<0.05$,
791 Student's t test)
792

793

FIGURE LEGENDS

FIG 1: Phenanthrene sorption isotherms (expressed as the quantity of PHE adsorbed on the solid phase Q_{ads}, relative to the concentration of PHE in solution at the equilibrium C_{eq}) at 25°C with and without rhamnolipids (0.55 $g.L^{-1}$) for (a) PPY soil and (b) Pv soil.

FIG 2: PHE degradation on PPY and Pv soils in the presence (at 300 $mg.kg^{-1}$) and absence of rhamnolipids in microcosms spiked with ^{13}C PHE (at 300 $mg.kg^{-1}$). DT20 and DT90 corresponding respectively to 20% and 90% of PHE dissipation are represented for both soils.

FIG 3: Quantification of bacterial 16S rRNA gene copies in the 12 fractions separated by CsCl gradients using real-time quantitative PCR. Data are presented for the two studied soils (PPY and Pv) with and without rhamnolipids and at DT90. Fractions n°3 and n°7 were selected for light DNA and heavy DNA sequencing and analyses, respectively.

FIG 4: Factorial correspondence analysis (FCA) of the relative proportion of the main OTUs (top 100) present in the (a) PPY and (b) Pv samples. Full-tone graphic patterns correspond to microcosms with rhamnolipids. For each soil type the principal component axes F1 and F2 explain most of the variance in the data cumulatively.

815 **Figure 1**

816

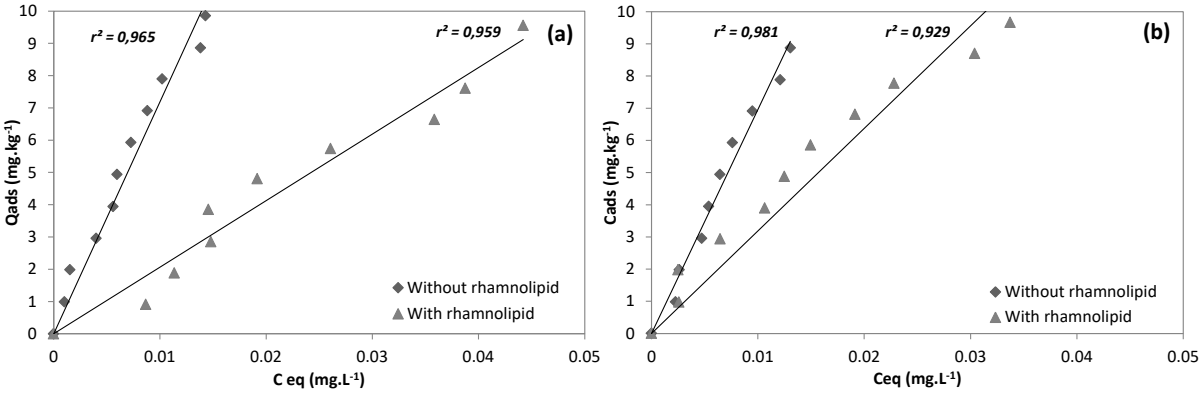

817

818

819 **Figure 2**

820

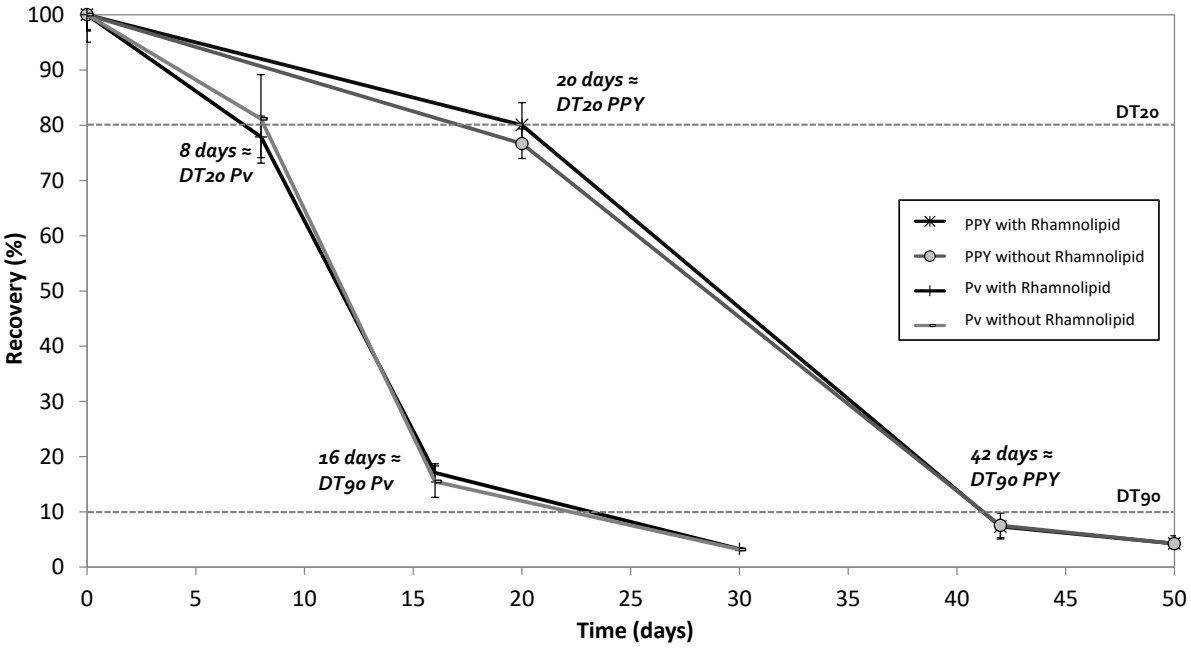

821

822

823 **Figure 3**

824

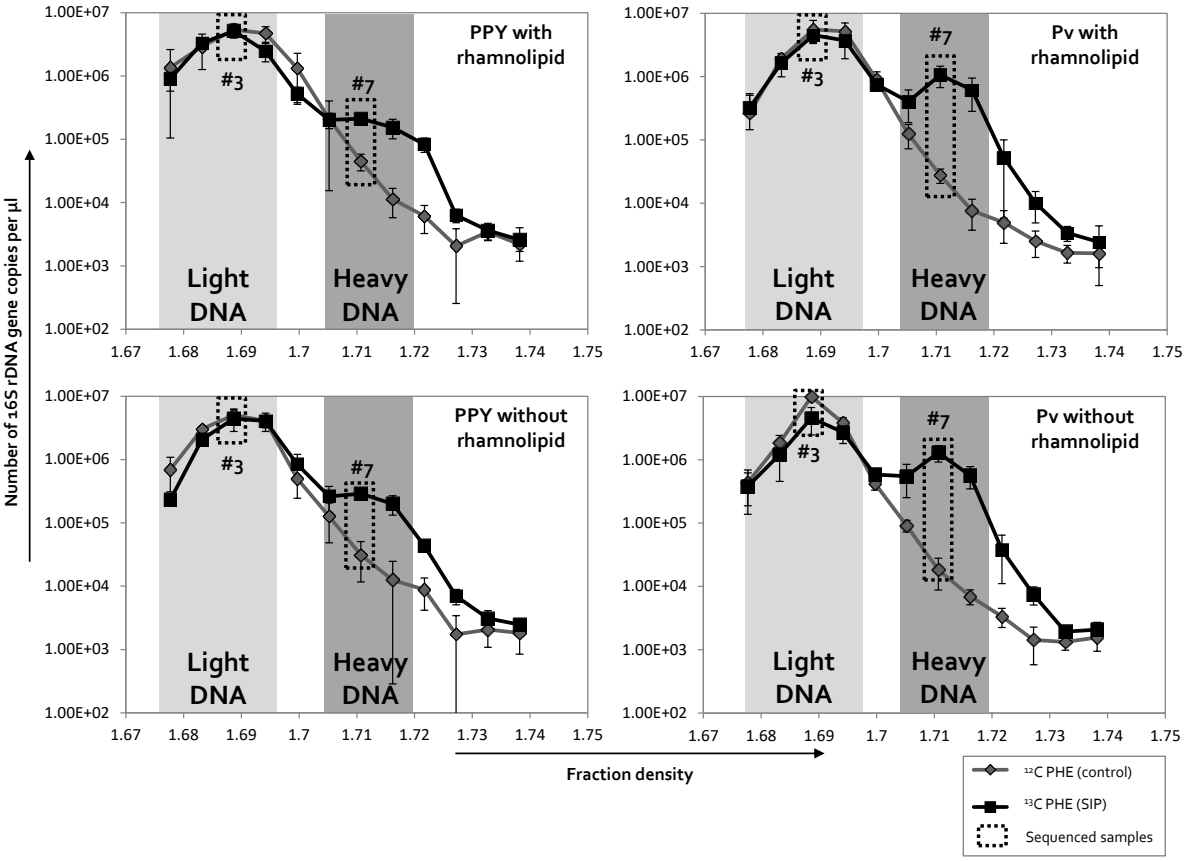

825

826

827 **Figure 4**

828

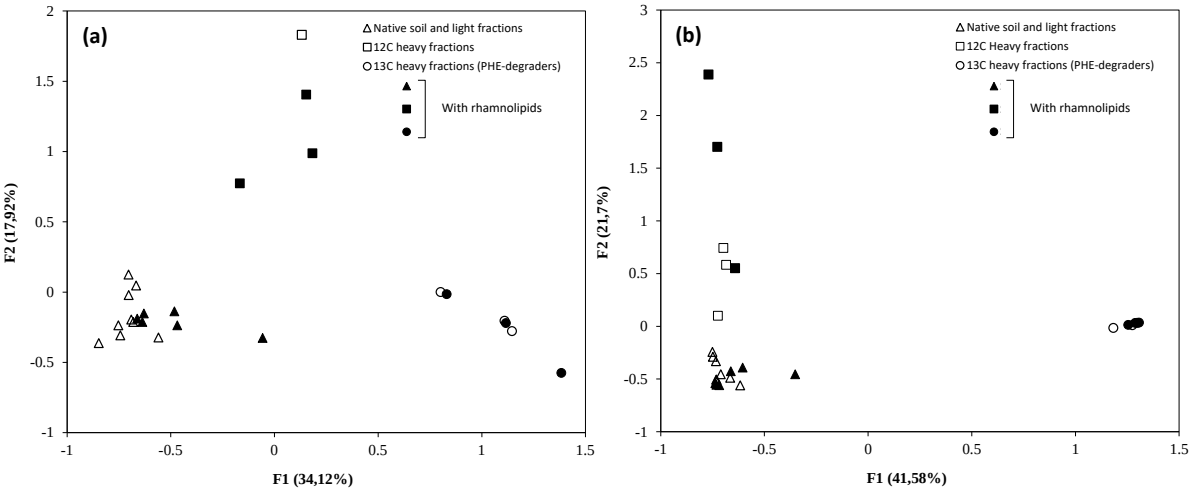

829

830

831

Supplemental materials

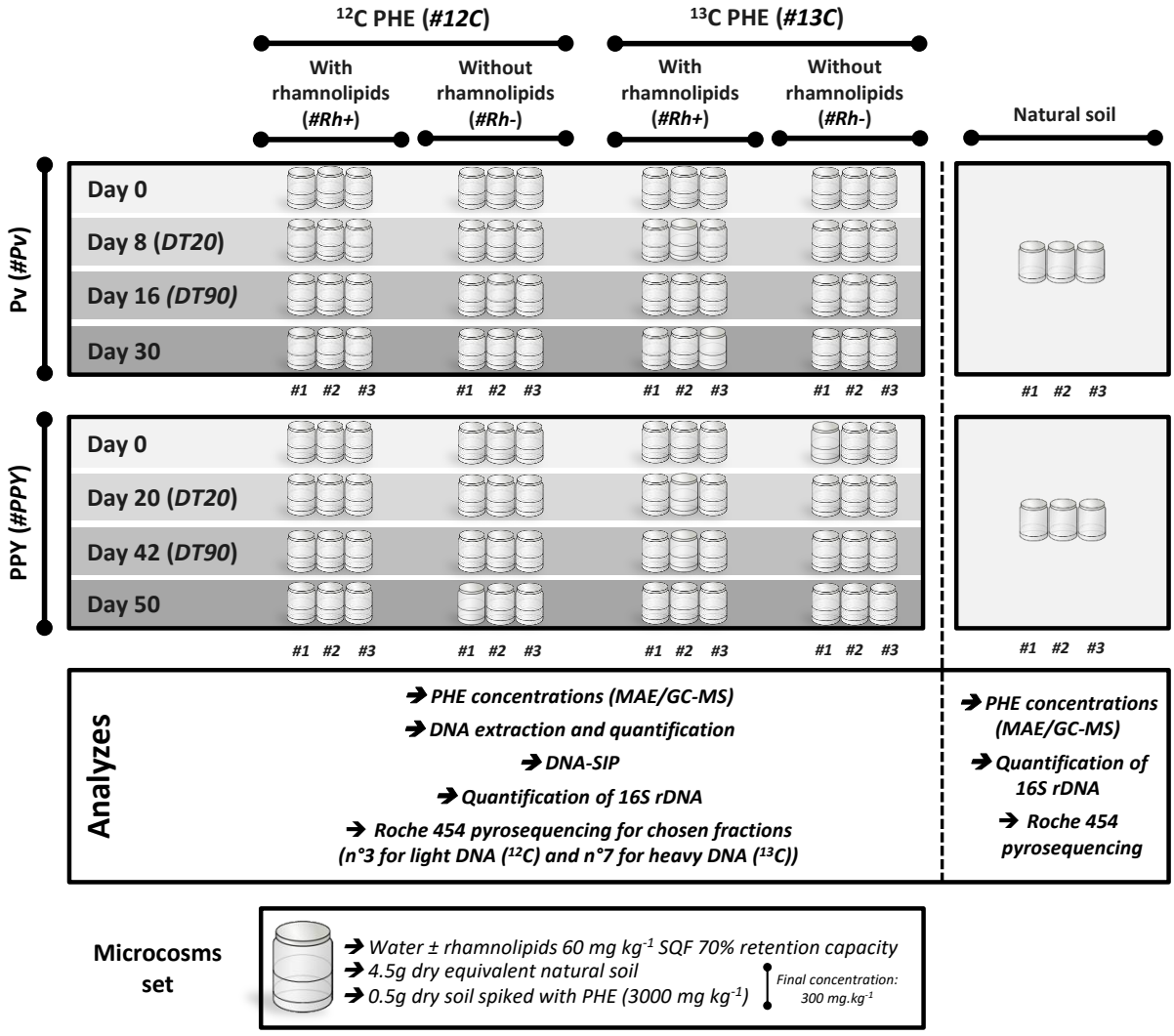

FIG S1: Experimental set up corresponding to the phenanthrene-contaminated microcosms.

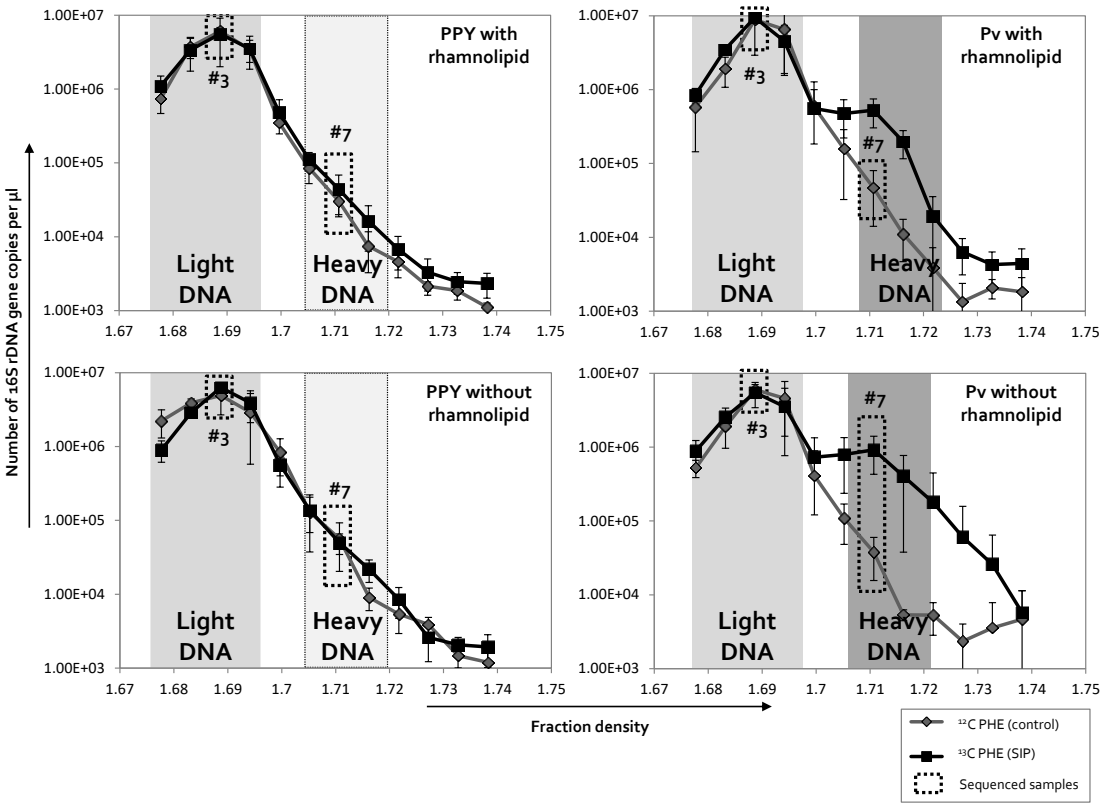

FIG S2: Quantification of bacterial 16S rRNA gene copies in the 12 fractions separated by CsCl gradients using real-time quantitative PCR. Data are presented for the two studied soils (PPY and Pv) with and without rhamnolipids and at DT20. Fractions n°3 and n°7 were selected as models for light DNA and heavy DNA containing fractions, respectively.

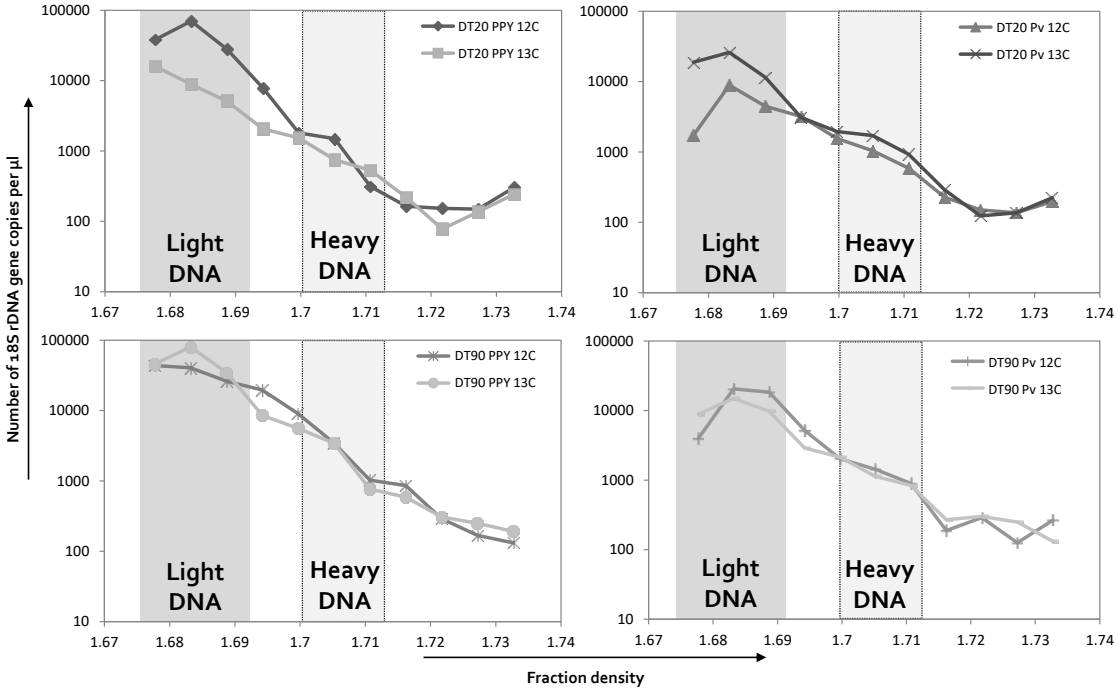

FIG S3: Quantification of fungal 18S rRNA gene copies in the 12 fractions separated by CsCl gradients using real-time quantitative PCR. Data are presented for the two studied soils (PPY and Pv) with rhamnolipids, at DT20 and DT90, only for one replicate.

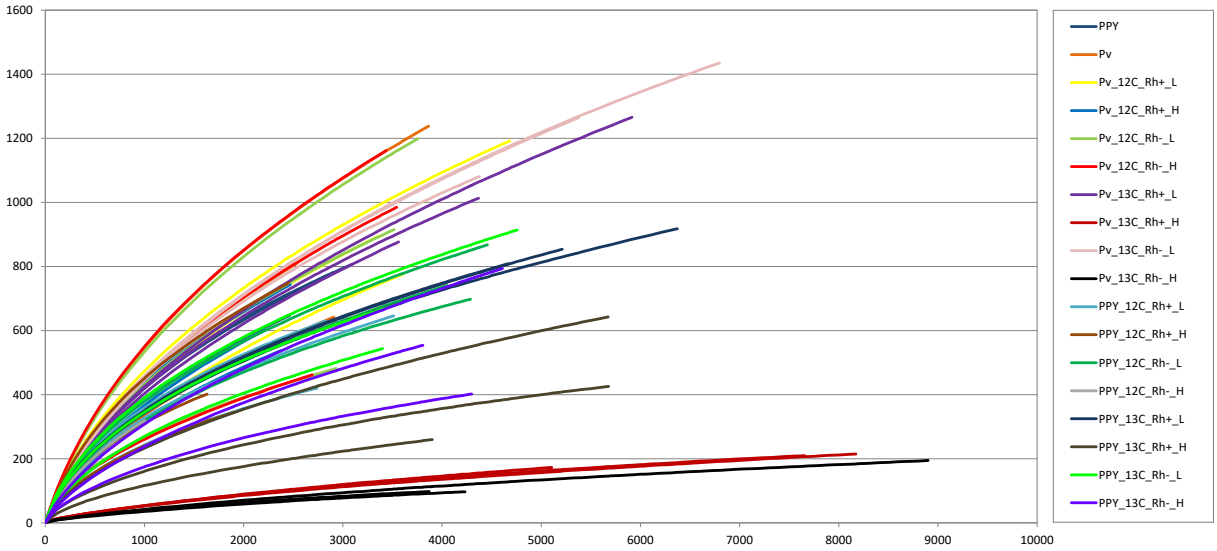

FIG S4: Rarefaction curves based on OTU at 97% similarity. Sequencing of 16S rDNA from light (L) and heavy (H) DNA fractions (n°3 and n°7, respectively) isolated from soils (Pv and PPY) incubated with ^{12}C or ^{13}C-PHE, and with and without rhamnolipids (Rh+ and Rh-). For each sample, triplicates are represented.

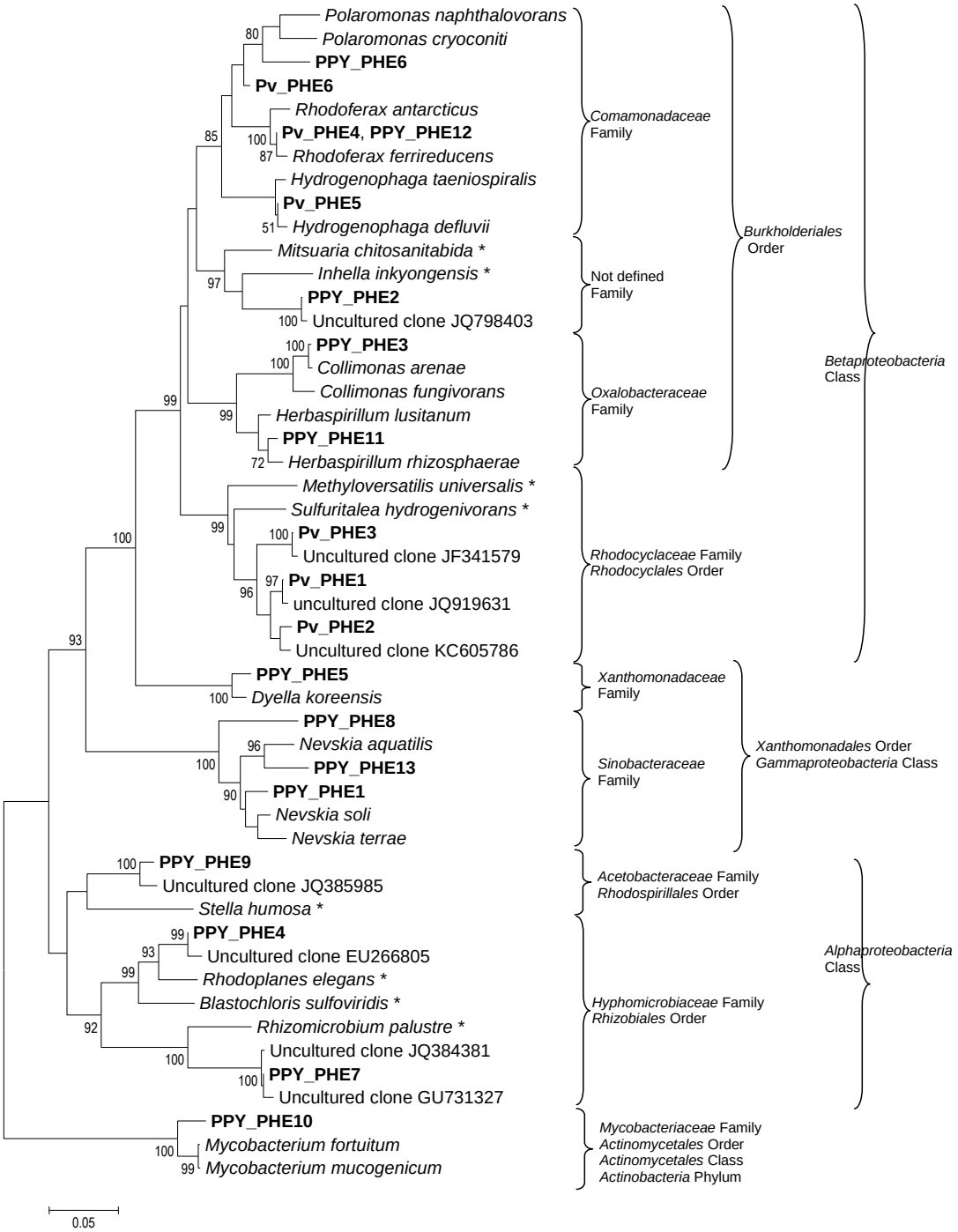

FIG S5: 16S rRNA gene phylogeny of the dominant PHE-degrading bacteria from soil microcosms enriched with PHE. Sequences of closest relative bacteria are included in the analysis. The unrooted dendrogram was generated using neighbor joining analysis. The scale bar corresponds to 0.05 substitutions per nucleotide position. Numbers on tree branches indicate bootstrap for those branches having >80% support. Sequences provided in this study are in bold.

866